
SOAPIA: Siamese-Guided Generation of Off-Target-Avoiding Protein Interactions with High Target Affinity

Anonymous Author(s)

Affiliation

Address

email

Abstract

Therapeutic molecules must selectively interact with a target protein while avoiding structurally or functionally similar off-targets. However, no existing generative strategy explicitly optimizes both target affinity and off-target avoidance. To address this, we introduce **SOAPIA**, a framework for the Siamese-guided generation of **Off-target-Avoiding Protein Interactions** with high target **Affinity**. SOAPIA generates *de novo* peptide binders by steering the generative process of a Diffusion Protein Language Model (DPLM) using a multi-objective Monte Carlo Tree Search (MCTS). Affinity is optimized via a pre-trained predictor, while specificity is enforced using a Siamese model trained with an adaptive Log-Sum-Exp Decoy Loss. This dual-guidance scheme enables Pareto-efficient exploration of discrete sequence space without gradient access. In benchmarks across 18 fusion oncoproteins, SOAPIA consistently identifies binders with strong affinity and high selectivity. In a targeted case study, SOAPIA generated a peptide that preferentially binds DHRSX::RPS4Y1 by engaging both the head and tail domains of the fusion while avoiding the wild-type counterparts. These results underscore SOAPIA’s promise for designing safe, specific biologics for fusion-driven cancers and other rare, currently untreatable diseases.

1 Introduction

Selective modulation of pathogenic proteins is essential for drug design [Nada et al., 2024]. Off-target interactions can reduce efficacy or lead to toxicity, a challenge shared across small molecules, PROTACs, and biologics [Garon et al., 2017, Chen et al., 2023a]. Since large-scale *in vitro* screening is costly and impractical, computational methods for designing drug-target interactions (DTIs) and protein-protein interactions (PPIs) are increasingly important. Structure-based approaches offer atomistic resolution but fail on disordered and chimeric proteins and are too slow for high-throughput design [Chen et al., 2023a]. Sequence-based models for DTIs [Singh et al., 2023, McNutt et al., 2024, Gao et al., 2024], PPIs [Sledzieski et al., 2021, Singh et al., 2022], and peptide design [Bhat et al., 2025, Tang et al., 2025] address this limitation by operating directly on primary sequences.

Yet, most generative approaches optimize only for target binding, without explicitly avoiding off-target interactions. This is particularly problematic for fusion oncoproteins, which drive many pediatric cancers and result from chromosomal translocations, often retaining high sequence identity with their wild-type head and tail domains [Vincoff et al., 2025]. Designing binders for such targets requires a multi-objective formulation that simultaneously maximizes affinity and enforces specificity—not just against a generic background proteome, but against multiple known off-targets. Including two explicit decoys during training and generation better reflects real-world therapeutic constraints, where safe and selective binding is essential [Chen et al., 2023a].

Discrete diffusion models have become a powerful class of generative frameworks for sequence design, enabling high-quality, controllable generation at the token level without requiring 3D structures or continuous embeddings [Campbell et al., 2024, Shi et al., 2024, Sahoo et al., 2024]. These models have recently shown strong performance in protein design tasks; as examples, DPLM [Wang et al., 2024] and EvoDiff [Alamdari et al., 2023] support structure-free generation of valid, foldable protein sequences. Most recently, PepTune [Tang et al., 2025] extended this paradigm to multi-objective optimization by introducing a Monte Carlo Tree Search (MCTS) framework that guides discrete diffusion using multiple non-differentiable reward functions. Operating in therapeutic peptide SMILES space, PepTune demonstrates that MCTS can efficiently explore the denoising landscape to discover Pareto-optimal solutions, even in the absence of gradient signals [Tang et al., 2025].

We build on these insights with **SOAPIA**: a framework for the Siamese-guided generation of **Off-target-Avoiding Protein Interactions with high Affinity**. SOAPIA combines a contrastive Siamese protein language model—trained with an adaptive Log-Sum-Exp Decoy Loss to separate binders from multiple off-targets—with a pre-trained affinity predictor. These soft-value signals define a dual-objective reward function that guides a Pareto-aware MCTS over the denoising trajectory of DPLM [Wang et al., 2024], enabling efficient sampling of short protein sequences that satisfy both constraints. We show that SOAPIA outperforms Best-of-N sampling baselines on both affinity and specificity and generates peptide-like binders that preferentially dock to fusion proteins while avoiding their head and tail domains. *In silico* docking with AlphaFold-Multimer [Evans et al., 2021] confirms SOAPIA’s ability to design safe and selective binders for undruggable and isoform-sensitive targets, such as fusion oncoproteins.

2 Methods

Data curation and handling All data curation, splitting, and clustering details can be found in the Supplementary Methods.

Protein encoding We encode four protein sequences—a binder, target, and two off-targets—into a shared latent space using the 33-layer ESM-2-650M model. The final two layers are unfrozen during training. A positional multi-head attention module ($n_heads = 10$) with rotary positional embeddings (RoPE) [Su et al., 2024] captures sequence-order information. Outputs are passed through two SiLU-activated linear layers with skip connections, and attention pooling produces fixed-length embeddings (Figure A1).

Specificity loss To enforce off-target avoidance, we train a Siamese model using an Adaptive Log-Sum-Exp Decoy Loss. Let \mathbf{b} , \mathbf{t} , \mathbf{ot}_1 , and \mathbf{ot}_2 represent the embeddings of the binder, target, and two off-targets. The loss is:

$$\mathcal{L} = \sum_{\mathbf{b}} \max \left(0, \text{dist}(\mathbf{b}, \mathbf{t}) - \frac{1}{\beta} \log \left(e^{\beta \cdot \text{dist}(\mathbf{b}, \mathbf{ot}_1)} + e^{\beta \cdot \text{dist}(\mathbf{b}, \mathbf{ot}_2)} + \epsilon \right) + \alpha \right) \quad (1)$$

where β controls sharpness, α is a margin, and $\epsilon = 10^{-8}$ ensures numerical stability.

Implementation details All models were implemented using PyTorch Lightning [Falcon, 2019] and trained on 4xA100 NVIDIA GPUs with an effective batch size of 128. Learning rate was initialized at 1×10^{-4} and decayed using cosine annealing with 200 warmup steps. Training was stopped after loss plateaued for three epochs (10 total). See Table A2 for full hyperparameters.

Embedding separation visualization After each epoch, we computed Euclidean distances between binder-target, binder-off-target 1, and binder-off-target 2 embeddings across the training set, and visualized them using matplotlib v3.8.2 (Figure A2).

Binder recovery screen To test specificity, 50,000 random amino acid sequences (lengths 56–856) were generated per target and scored using the Siamese model. The true binder was ranked by:

$$D = \text{dist}(\mathbf{b}, \mathbf{t}) - \frac{1}{\beta} \log \left(e^{\beta \cdot \text{dist}(\mathbf{b}, \mathbf{ot}_1)} + e^{\beta \cdot \text{dist}(\mathbf{b}, \mathbf{ot}_2)} + \epsilon \right) + \alpha \quad (2)$$

79 Lower D implies better specificity. Rankings were evaluated across multiple thresholds (Figure A3).

80 **Masked discrete diffusion** Binder generation is based on a masked discrete diffusion model
 81 (MDM) [Sahoo et al., 2024, Shi et al., 2024, Campbell et al., 2024]. The forward process corrupts a
 82 clean sequence \mathbf{x}_0 with:

$$p_t(\mathbf{x}_t|\mathbf{x}_0) = \prod_{i=1}^n \text{Cat}(x_t^i; \alpha_t \delta(x_0^i) + (1 - \alpha_t) \delta(m)), \quad (3)$$

83 and the reverse process denoises via:

$$p_t(x_{t-1}^i | x_t^i, x_0^i) \propto \alpha_{t-1} \delta(x_0^i) + (1 - \alpha_{t-1}) \delta(m). \quad (4)$$

84 Training minimizes weighted cross-entropy:

$$\mathcal{L} = -\mathbb{E}_{\mathbf{x}_t \sim p_t} \sum_{i=1}^n x_0^i \log \mu_\theta(x_t^i, t). \quad (5)$$

85 **Sampling and generation strategies (SOAPIA)** SOAPIA generates peptide binders by applying
 86 MCTS over the denoising trajectory of DPLM [Wang et al., 2024], guided by two soft-value reward
 87 functions which are maximized for the optimal binder: one reward from the Siamese model trained for
 88 off-target avoidance as described here ($r(x) = -D$) (2), and one from a pre-trained peptide-protein
 89 affinity predictor Chen et al. [2025]. At each expansion step, candidate sequences are sampled from
 90 the DPLM transition distribution $p_\theta(x_{t-1} | x_t, t)$ and completed via ancestral decoding. Each fully
 91 unmasked sequence is scored along both objectives and compared to a dynamically updated Pareto
 92 frontier. Soft reward vectors—computed from overlap with frontier members—encourage exploration
 93 of diverse trade-offs, while heavily dominated sequences are pruned.

94 We evaluate multiple guidance mechanisms to direct sequence refinement, including SVDD [Li et al.,
 95 2024], which selects the best of m candidates at each step; simple guidance [Schiff et al., 2025],
 96 which applies reward-informed local updates; and NOS [Gruver et al., 2023], which performs iterative
 97 local search through the reward landscape. These samplers and guidance methods are combined
 98 with higher-level generation strategies. The *Basic* strategy generates N samples without filtering;
 99 *Best-of- N* selects the top N from a larger pool; *Scalarized Best-of- N* applies a weighted reward
 100 $R(x) = \lambda r_1(x) + (1 - \lambda) r_2(x)$; and *Pareto Best-of- N* returns non-dominated sequences. The *MCTS*
 101 strategies used by SOAPIA integrate sampling and guidance at each expansion and rollout step,
 102 updating the Pareto frontier online as sequences are generated. *MCTS* uses specificity scores only,
 103 while *MultiMCTS* performs multi-objective guidance with both specificity and affinity scores. See
 104 Algorithm 1 for details.

105 3 Results

106 **Siamese model results** First, we trained our Siamese model to obtain the specificity predictor used
 107 for SOAPIA’s dual-guided sampling. The model was trained to embed binders closer to their target
 108 than to either of two off-targets. The architecture is shown in Figure A1. Over the course of training,
 109 we observed progressive separation in the embedding space: binder–target distances decreased while
 110 binder–off-target distances increased, as shown in Figure A2. To assess its ranking performance, we
 111 evaluated the model against 50,000 randomly generated binders per test case. The true binder was
 112 ranked in the top-1 for 19.2% of cases and in the top-25% for 56.8% (Figure A3). Finally, protein
 113 role distributions across train, validation, and test splits are shown in Figure A4, confirming dataset
 114 diversity and generalization.

115 **Generation of specific, high-affinity peptides** SOAPIA successfully generates novel, short binding
 116 proteins with a variety of sampling strategies (Figure 1). When different methodologies were evaluated
 117 on 20 examples from the Siamese specificity model’s test set, *MultiMCTS* achieved the optimal
 118 results. Binders “passed” the specificity task if their reward scores were positive, indicating that the
 119 binder is embedded closer to the target than the two off-targets in the model’s latent space. For the
 120 affinity task, a passing threshold of 6.5 was selected, as indicated in MOG-DFM [Chen et al., 2025].
 121 All three guidance methods - NOS, simple, and SVDD - performed well in the expansion and rollout
 122 steps of *MultiMCTS*. Unguided generation was also competitive. NOS achieved the best results, with
 123 a dual-objective pass rate of 48.12%, and only 5.31% of generated samples failing to meet the criteria
 124 for either objective (Figure 1).

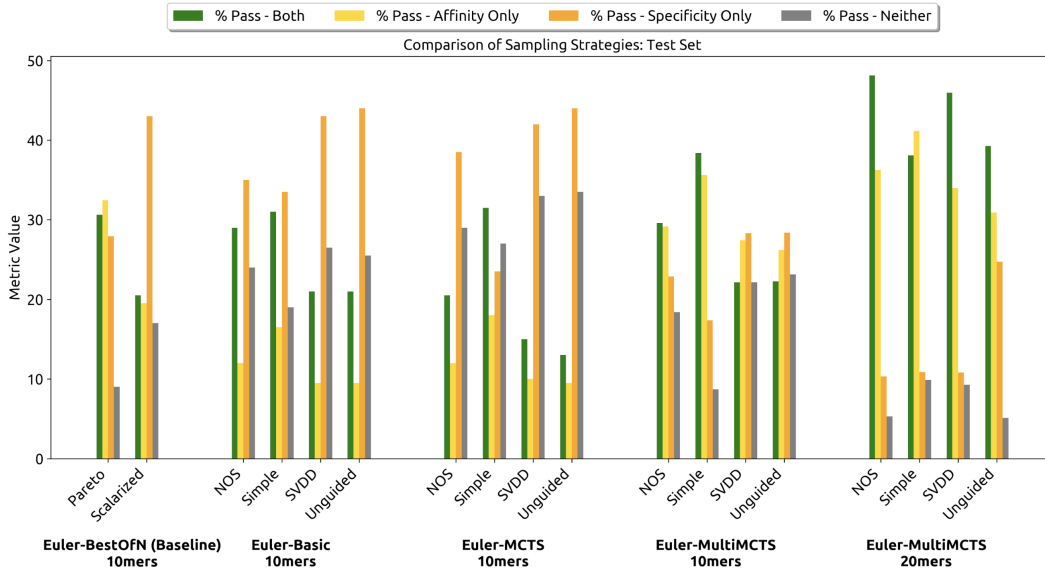


Figure 1: **Performance of different sampling strategies on the Siamese model test set.** The passing thresholds for specificity and affinity rewards are 0 and 6.5, respectively. For each input (target, off-target 1, and off-target 2), 10 novel binding peptides of length 10 or 20 were generated and scored.

Targeting fusion oncoproteins Next, we sought to determine whether SOAPIA can be applied to target proteins which have no known specific binders. We evaluated *MultiMCTS* on a set of 18 fusion oncoproteins, whose off-targets are their corresponding wild-type heads and tails (Figure 2). For all guidance strategies tested, the maximum specificity scores were greater than 12, indicating that very strong selectivity was achieved for the best samples. Similarly, the maximum affinity values were consistently strong, exceeding 8 in all cases. The mean affinity scores were greater than 7 for all methods, indicating that on average, SOAPIA-designed fusion oncoprotein binders pass the affinity criterion. The four strategies were slightly more differentiated in average specificity, with simple guidance achieving the highest value of 2.84 (Figure 2A). Accordingly, simple guidance also produced the highest simultaneous dual-objective hit rate of 68.27% (Figure 2B).

Targeting DHRX::RPS4Y1 as a case study To validate that SOAPIA’s rewards are meaningful, we co-folded one of the highest-scoring samples, with predicted specificity and affinity scores of 12.14 and 6.92 (sequence in Table A3). The target protein, DHRX::RSP4Y1, is implicated in pancreatic adenocarcinoma Vincoff et al. [2025]. When co-folded with the fusion, wild-type DHRX, and wild-type RPS4Y1 in AlphaFold-Multimer, our 20-amino-acid peptide achieved a much higher ipTM with the target (0.75) than either “off”-target (0.40, 0.39 respectively). Additionally, the predicted structure of the binder-target complex implies a selective binding mode, where the peptide engages both the head and tail portions of the fusion oncoprotein (Figure 3A). Meanwhile, when interacting with the wild-type head and tail proteins alone, the peptide largely fails to adopt a stable secondary structure (Figure 3B-C). In total, these findings demonstrate SOAPIA’s potential to design peptides that selectively recognize fusion oncoproteins while minimizing interactions with their wild-type counterparts.

4 Discussion

SOAPIA is a new framework for multi-objective binder design that jointly optimizes specificity and affinity using a Pareto-guided MCTS over a DPLM prior. Inspired by PepTune [Tang et al., 2025], SOAPIA combines soft-value signals from a Siamese contrastive model and a trained affinity predictor Chen et al. [2025] to guide tree-based exploration during denoising, without requiring gradient access to either objective. This dual-guidance mechanism allows SOAPIA to perform competitively against

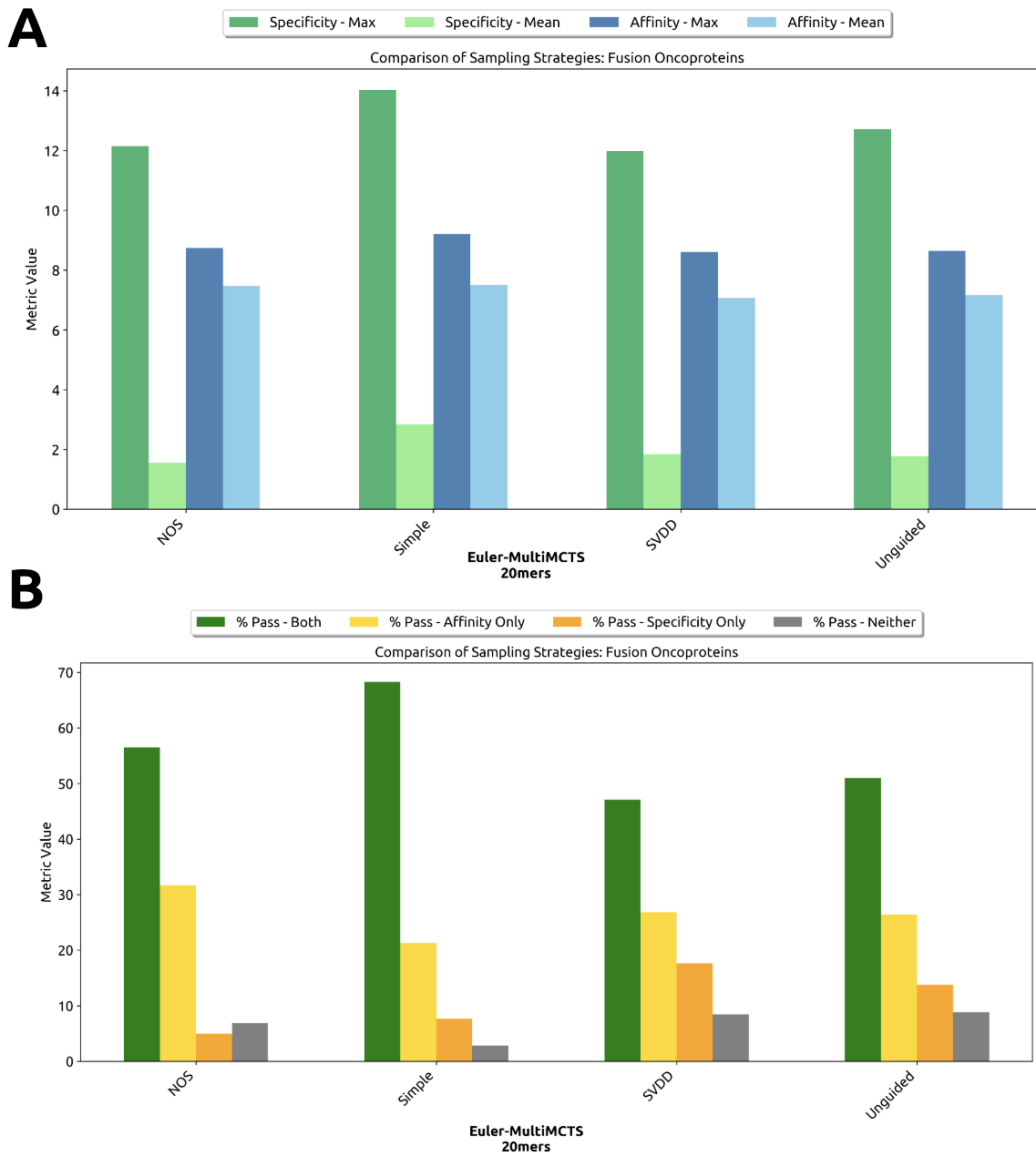


Figure 2: **Performance of different guidance methods with *MultiMCTS* on a set of fusion oncoproteins.** **A** Maximum and mean rewards across 10 samples per target, for 18 targets. **B** Pass rates for each objective across all generated samples.

Best-of-N sampling baselines across both objectives, generating peptide sequences that exhibit strong binding while avoiding homologous off-targets. Notably, SOAPIA is capable of generating binders to fusion oncoproteins that show preferential docking to the full fusion but not to the individual head or tail proteins. This level of selectivity is critical for therapeutic applications, particularly in pediatric fusion-driven cancers, where targeting the aberrant fusion protein while sparing wild-type counterparts is essential for minimizing toxicity Vincoff et al. [2025].

Looking ahead, we will refine SOAPIA’s guidance weights and rollout policies to further improve sample efficiency, and conduct experimental validation in cellular systems focused on disordered fusion oncoproteins. For this, we plan to integrate FusOn-pLM embeddings [Vincoff et al., 2025] to better capture breakpoint-localized context, and incorporate PTM-Mamba embeddings [Peng et al., 2025] to enable peptide design sensitive to post-translational modification states. In addition

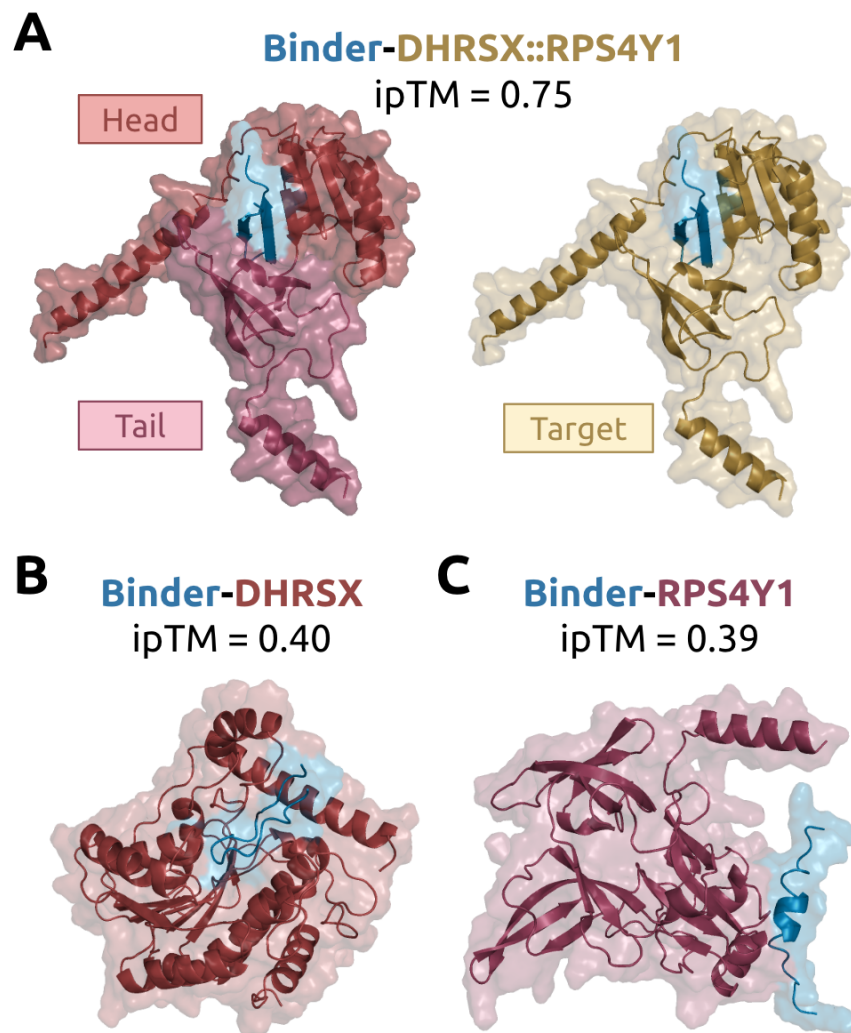


Figure 3: **AlphaFold-Multimer-predicted structures of top-performing binder to DHRXS::RPS4Y1.** **A** Binder with target protein DHRXS::RPS4Y1. **B-C** Binder with off-target 1 - head protein DHRXS (B), and off-target 2 - tail protein RPS4Y1 (C).

164 to MCTS, recent work on multi-objective guided flow matching (MOG-DFM [Chen et al., 2025])
 165 offers a potential alternative decoding framework for joint optimization in discrete sequence space.
 166 Finally, when paired with experimental platforms such as ubiquibodies (uAbs) and deubiquibodies
 167 (duAbs) for targeted protein degradation [Brix et al., 2023, Bhat et al., 2025, Chen et al., 2023b]
 168 and stabilization [Hong et al., 2025], SOAPIA provides a generalizable, programmable approach to
 169 modulating previously undruggable proteins, with potential impact across oncology, rare disease, and
 170 immunotherapy.

References

- Hossam Nada, Yongseok Choi, Sungdo Kim, Kwon Su Jeong, Nicholas A. Meanwell, and Kyeong Lee. New insights into protein–protein interaction modulators in drug discovery and therapeutic advance. *Signal Transduction and Targeted Therapy*, 9(1), December 2024. ISSN 2059-3635. doi: 10.1038/s41392-024-02036-3. URL <http://dx.doi.org/10.1038/s41392-024-02036-3>.
- Sarah L. Garon, Rebecca K. Pavlos, Katie D. White, Nancy J. Brown, Cosby A. Stone, and Elizabeth J. Phillips. Pharmacogenomics of off-target adverse drug reactions. *British Journal of Clinical Pharmacology*, 83(9):1896–1911, April 2017. ISSN 1365-2125. doi: 10.1111/bcp.13294. URL <http://dx.doi.org/10.1111/bcp.13294>.
- Tianlai Chen, Lauren Hong, Vivian Yudistyra, Sophia Vincoff, and Pranam Chatterjee. Generative design of therapeutics that bind and modulate protein states. *Current Opinion in Biomedical Engineering*, 28:100496, December 2023a. ISSN 2468-4511. doi: 10.1016/j.cobme.2023.100496. URL <http://dx.doi.org/10.1016/j.cobme.2023.100496>.
- Rohit Singh, Samuel Sledzieski, Bryan Bryson, Lenore Cowen, and Bonnie Berger. Contrastive learning in protein language space predicts interactions between drugs and protein targets. *Proceedings of the National Academy of Sciences*, 120(24):e2220778120, 2023.
- Andrew T McNutt, Abhinav K Adduri, Caleb N Ellington, Monica T Dayao, Eric P Xing, Hosein Mohimani, and David R Koes. Sprint enables interpretable and ultra-fast virtual screening against thousands of proteomes. *arXiv preprint arXiv:2411.15418*, 2024.
- Bowen Gao, Bo Qiang, Haichuan Tan, Yinjun Jia, Minsi Ren, Minsi Lu, Jingjing Liu, Wei-Ying Ma, and Yanyan Lan. Drugclip: Contrastive protein-molecule representation learning for virtual screening. *Advances in Neural Information Processing Systems*, 36, 2024.
- Samuel Sledzieski, Rohit Singh, Lenore Cowen, and Bonnie Berger. D-script translates genome to phenome with sequence-based, structure-aware, genome-scale predictions of protein-protein interactions. *Cell Systems*, 12(10):969–982, 2021.
- Rohit Singh, Kapil Devkota, Samuel Sledzieski, Bonnie Berger, and Lenore Cowen. Topsy-turvy: integrating a global view into sequence-based ppi prediction. *Bioinformatics*, 38(Supplement_1): i264–i272, 2022.
- Suhaas Bhat, Kalyan Palepu, Lauren Hong, Joey Mao, Tianzheng Ye, Rema Iyer, Lin Zhao, Tianlai Chen, Sophia Vincoff, Rio Watson, Tian Z. Wang, Divya Sri Jay, Venkata Srikar Kavirayuni, Kseniia Kholina, Shrey Goel, Pranay Vure, Aniruddha J. Deshpande, Scott H. Soderling, Matthew P. DeLisa, and Pranam Chatterjee. De novo design of peptide binders to conformationally diverse targets with contrastive language modeling. *Science Advances*, 11(4), January 2025. ISSN 2375-2548. doi: 10.1126/sciadv.adr8638. URL <http://dx.doi.org/10.1126/sciadv.adr8638>.
- Sophia Tang, Yinuo Zhang, and Pranam Chatterjee. Peptune: De novo generation of therapeutic peptides with multi-objective-guided discrete diffusion. *Proceedings of the 42nd International Conference on Machine Learning (ICML)*, 2025.
- Sophia Vincoff, Shrey Goel, Kseniia Kholina, Rishab Pulugurta, Pranay Vure, and Pranam Chatterjee. Fuson-plm: a fusion oncoprotein-specific language model via adjusted rate masking. *Nature Communications*, 16(1), February 2025. ISSN 2041-1723. doi: 10.1038/s41467-025-56745-6. URL <http://dx.doi.org/10.1038/s41467-025-56745-6>.
- Andrew Campbell, Jason Yim, Regina Barzilay, Tom Rainforth, and Tommi Jaakkola. Generative flows on discrete state-spaces: enabling multimodal flows with applications to protein co-design. In *Proceedings of the 41st International Conference on Machine Learning, ICML’24*. JMLR.org, 2024.
- Jiaxin Shi, Kehang Han, Zhe Wang, Arnaud Doucet, and Michalis K. Titsias. Simplified and generalized masked diffusion for discrete data. In *Advances in Neural Information Processing Systems*, 2024.

219 Subham Sekhar Sahoo, Marianne Arriola, Yair Schiff, Aaron Gokaslan, Edgar Marroquin, Justin T
220 Chiu, Alexander Rush, and Volodymyr Kuleshov. Simple and effective masked diffusion language
221 models. *arXiv preprint arXiv:2406.07524*, 2024.

222 Xinyou Wang, Zaixiang Zheng, Fei Ye, Dongyu Xue, Shujian Huang, and Quanquan Gu. Diffusion
223 language models are versatile protein learners. *arXiv preprint arXiv:2402.18567*, 2024.

224 Sarah Alamdari, Nitya Thakkar, Rianne van den Berg, Neil Tenenholtz, Bob Strome, Alan Moses,
225 Alex Xijie Lu, Nicolo Fusi, Ava Pardis Amini, and Kevin K Yang. Protein generation with
226 evolutionary diffusion: sequence is all you need. *BioRxiv*, pages 2023–09, 2023.

227 Richard Evans, Michael O’Neill, Alexander Pritzel, Natasha Antropova, Andrew Senior, Tim Green,
228 Augustin Židek, Russ Bates, Sam Blackwell, Jason Yim, Olaf Ronneberger, Sebastian Bodenstein,
229 Michal Zielinski, Alex Bridgland, Anna Potapenko, Andrew Cowie, Kathryn Tunyasuvunakool,
230 Rishub Jain, Ellen Clancy, Pushmeet Kohli, John Jumper, and Demis Hassabis. Protein complex
231 prediction with alphafold-multimer. October 2021. doi: 10.1101/2021.10.04.463034. URL
232 <http://dx.doi.org/10.1101/2021.10.04.463034>.

233 Jianlin Su, Murtadha Ahmed, Yu Lu, Shengfeng Pan, Wen Bo, and Yunfeng Liu. Roformer: Enhanced
234 transformer with rotary position embedding. *Neurocomputing*, 568:127063, 2024.

235 William A Falcon. Pytorch lightning. *GitHub*, 3, 2019.

236 Tong Chen, YINUO Zhang, Sophia Tang, and Pranam Chatterjee. Multi-objective-guided discrete flow
237 matching for controllable biological sequence design. *arXiv preprint arXiv:2505.07086*, 2025.

238 Xiner Li, Yulai Zhao, Chenyu Wang, Gabriele Scalia, Gokcen Eraslan, Surag Nair, Tommaso
239 Biancalani, Shuiwang Ji, Aviv Regev, Sergey Levine, and Masatoshi Uehara. Derivative-free
240 guidance in continuous and discrete diffusion models with soft value-based decoding, 2024. URL
241 <https://arxiv.org/abs/2408.08252>.

242 Yair Schiff, Subham Sekhar Sahoo, Hao Phung, Guanghan Wang, Sam Boshar, Hugo Dalla-torre,
243 Bernardo P. de Almeida, Alexander Rush, Thomas Pierrot, and Volodymyr Kuleshov. Simple
244 guidance mechanisms for discrete diffusion models, 2025.

245 Nate Gruver, Samuel Stanton, Nathan C. Frey, Tim G. J. Rudner, Isidro Hotzel, Julien Lafrance-
246 Vanasse, Arvind Rajpal, Kyunghyun Cho, and Andrew Gordon Wilson. Protein design with guided
247 discrete diffusion, 2023. URL <https://arxiv.org/abs/2305.20009>.

248 Fred Zhangzhi Peng, Chentong Wang, Tong Chen, Benjamin Schussheim, Sophia Vincoff, and
249 Pranam Chatterjee. Ptm-mamba: a ptm-aware protein language model with bidirectional gated
250 mamba blocks. *Nature Methods*, 22(5):945–949, April 2025. ISSN 1548-7105. doi: 10.1038/
251 s41592-025-02656-9. URL <http://dx.doi.org/10.1038/s41592-025-02656-9>.

252 Garyk Brixi, Tianzheng Ye, Lauren Hong, Tian Wang, Connor Monticello, Natalia Lopez-Barbosa,
253 Sophia Vincoff, Vivian Yudistyra, Lin Zhao, Elena Haarer, Tianlai Chen, Sarah Pertsemlidis,
254 Kalyan Palepu, Suhaas Bhat, Jayani Christopher, Xinning Li, Tong Liu, Sue Zhang, Lillian
255 Petersen, Matthew P. DeLisa, and Pranam Chatterjee. Salt&pepr is an interface-predicting
256 language model for designing peptide-guided protein degraders. *Communications Biology*, 6(1),
257 October 2023. ISSN 2399-3642. doi: 10.1038/s42003-023-05464-z. URL <http://dx.doi.org/10.1038/s42003-023-05464-z>.

258

259 Tianlai Chen, Madeleine Dumas, Rio Watson, Sophia Vincoff, Christina Peng, Lin Zhao, Lauren
260 Hong, Sarah Pertsemlidis, Mayumi Shapers-Cheu, Tian Zi Wang, Divya Srijay, Connor Mon-
261 ticello, Pranay Vure, Rishab Pulugurta, Kseniia Kholina, Shrey Goel, Matthew P. DeLisa, Ray
262 Truant, Hector C. Aguilar, and Pranam Chatterjee. Pepmlm: Target sequence-conditioned gen-
263 eration of therapeutic peptide binders via span masked language modeling. *arXiv*, 2023b. doi:
264 10.48550/ARXIV.2310.03842. URL <https://arxiv.org/abs/2310.03842>.

265 Lauren Hong, Tianzheng Ye, Tian Z. Wang, Divya Srijay, Howard Liu, Lin Zhao, Rio Watson,
266 Sophia Vincoff, Tianlai Chen, Kseniia Kholina, Shrey Goel, Matthew P. DeLisa, and Pranam
267 Chatterjee. Programmable protein stabilization with language model-derived peptide guides.
268 *Nature Communications*, 16(1), April 2025. ISSN 2041-1723. doi: 10.1038/s41467-025-58872-6.
269 URL <http://dx.doi.org/10.1038/s41467-025-58872-6>.

- 270 Rose Oughtred, Jennifer Rust, Christie Chang, Bobby-Joe Breitkreutz, Chris Stark, Andrew Willems,
271 Lorrie Boucher, Genie Leung, Nadine Kolas, Frederick Zhang, et al. The biogrid database: A
272 comprehensive biomedical resource of curated protein, genetic, and chemical interactions. *Protein*
273 *Science*, 30(1):187–200, 2021.
- 274 Noemi Del Toro, Anjali Shrivastava, Eliot Ragueneau, Birgit Meldal, Colin Combe, Elisabet Barrera,
275 Livia Perfetto, Karyn How, Prashansa Ratan, Gautam Shirodkar, et al. The intact database: efficient
276 access to fine-grained molecular interaction data. *Nucleic acids research*, 50(D1):D648–D653,
277 2022.
- 278 Anton Bushuiev, Roman Bushuiev, Anatolii Filkin, Petr Kouba, Marketa Gabrielova, Michal Gabriel,
279 Jiri Sedlar, Tomas Pluskal, Jiri Damborsky, Stanislav Mazurenko, et al. Learning to design
280 protein-protein interactions with enhanced generalization. *arXiv preprint arXiv:2310.18515*, 2023.
- 281 Philipp Blohm, Goar Frishman, Pawel Smialowski, Florian Goebels, Benedikt Wachinger, Andreas
282 Ruepp, and Dmitrij Frishman. Negatome 2.0: a database of non-interacting proteins derived by
283 literature mining, manual annotation and protein structure analysis. *Nucleic acids research*, 42
284 (D1):D396–D400, 2014.
- 285 Zeming Lin, Halil Akin, Roshan Rao, Brian Hie, Zhongkai Zhu, Wenting Lu, Nikita Smetanin,
286 Robert Verkuil, Ori Kabeli, Yaniv Shmueli, et al. Evolutionary-scale prediction of atomic-level
287 protein structure with a language model. *Science*, 379(6637):1123–1130, 2023.
- 288 Martin Steinegger and Johannes Söding. Mmseqs2 enables sensitive protein sequence searching for
289 the analysis of massive data sets. *Nature biotechnology*, 35(11):1026–1028, 2017.

290 A Algorithm

Algorithm 1 SOAPIA: Pareto-Guided MCTS with Dual Objective Scoring

```

1: Input: Denoising model  $p_\theta(x_{t-1} \mid x_t, t)$ , specificity model  $f_{\text{spec}}(x)$ , affinity model  $f_{\text{aff}}(x)$ , number of
   MCTS iterations  $N_{\text{mcts}}$ , number of children  $N_{\text{child}}$ 
2: Output: Pareto frontier of guided binders  $\mathcal{P}^*$ 
3: Initialize:  $x_T \leftarrow [M]^L$  (fully masked),  $\mathcal{P}^* \leftarrow \{\}$ ,  $t \leftarrow T$ 
4: for  $i = 1$  to  $N_{\text{mcts}}$  do
5:   Selection:  $x_{\text{leaf}} \leftarrow \text{SELECTLEAF}(x_T)$ 
6:   Expansion:
7:     for  $j = 1$  to  $N_{\text{child}}$  do
8:       Sample  $x_{t-1}^{(j)} \sim p_\theta(\cdot \mid x_{\text{leaf}}, t)$ 
9:       Unmask  $k$  positions to form  $x_{\text{child}}^{(j)}$ 
10:      Add  $x_{\text{child}}^{(j)}$  to  $\text{children}(x_{\text{leaf}})$ 
11:    end for
12:    Rollout:
13:      for each  $x_{\text{child}}^{(j)}$  do
14:         $\tilde{x}^{(j)} \leftarrow \text{ROLLOUTTOCOMPLETION}(x_{\text{child}}^{(j)})$ 
15:        Compute scores:  $\mathbf{s}^{(j)} \leftarrow [f_{\text{spec}}(\tilde{x}^{(j)}), f_{\text{aff}}(\tilde{x}^{(j)})]$ 
16:        Compute soft reward vector:  $\mathbf{r}^{(j)} \leftarrow \text{MULTICOMPAREPARETOFRONT}(\tilde{x}^{(j)}, \mathbf{s}^{(j)}, \text{tokens})$ 
17:        Update  $\mathcal{P}^*$  with  $\tilde{x}^{(j)}$  if non-dominated
18:      end for
19:      Backpropagation:  $\text{BACKPROPAGATE}(x_{\text{leaf}}, \{\mathbf{r}^{(j)}\})$ 
20:    end for
21: return  $\mathcal{P}^*$ 

```

291 B Supplementary Methods

292 B.1 Data collection

293 Each sample in the training data is a protein quadruplet consisting of a binder, target, off-target 1,
294 and off-target 2. Positive protein-protein interactions (PPIs) were collected from BioGRID (October
295 2022) [Oughtred et al., 2021], IntAct (October 2022) [Del Toro et al., 2022], and PPIRef (January
296 2025) [Bushuiev et al., 2023]. Negative interactions were collected from Negatome2.0 [Blohm et al.,
297 2014], a manually curated database of proteins with experimental evidence indicating the absence of
298 direct interaction. Positive PPIs were filtered by cleaning (e.g. dropping sequences with non-natural
299 amino acids), swapping targets and binders to double the dataset size, removing duplicate homomer
300 interactions, applying a length limit of 1022 amino acids for both target and binder sequences, and
301 only retaining rows where one partner is included in the Negatome. The Negatome was filtered by
302 removing any listed target and off-target pairs that are included as binder and target pairs in the PPI
303 database. This produced a dataset of 245,587 positive PPIs and 7,198 negative interactions.

304 B.2 Quadruplet selection

305 The training, validation, and testing datasets were designed to (1) enhance generalizability by
306 including diverse binders, targets, and off-targets, (2) prevent rigid role assignments by allowing
307 any sequence to act in any interaction context, and (3) maximize difficulty to improve learning.
308 Quadruplet selection was formulated as a linear programming problem using length-averaged ESM-2-
309 650M [Lin et al., 2023] embeddings. With PuLP v2.9.0, quadruplets were optimized for difficulty
310 while minimizing role repetition (Supplementary Algorithm ??). Difficulty increased with higher
311 cosine similarity between target and off-target embeddings, ensuring the Siamese model learned to
312 distinguish subtle differences. Euclidean distance was used in the loss function, but cosine similarity
313 was preferred for selection due to its bounded range (-1 to 1). Selecting closely related targets
314 and off-targets better reflects SOAPIA’s real-world applications, such as designing binders that avoid
315 wild-type protein interactions. To ensure the model learned relationships rather than predefined roles,
316 four constraints were imposed: (1) each binder appears at most ten times, (2) each target-off-target
317 grouping appears only once, (3) each target appears once per binder, and (4) each off-target appears

318 once per binder. Constraint 1 was pre-enforced by subsampling positive PPIs, and Constraint 2
319 required a tiebreaker term ($\lambda = 0.001$) based on Euclidean binder-target distance. A total of 1,352
320 quadruplets were selected, consisting of 565 unique binders, 1,054 targets, and 969 off-targets.

321 **B.3 Clustering and splitting**

322 Quadruplets were clustered on binder sequence using MMSeqs2 easy clustering module [Steinegger
323 and Söding, 2017] with a minimum sequence identity of 30% and a coverage threshold of 70%. The
324 resulting clusters were randomly split at 80-10-10 ratio using `sklearn v1.2.0` into a training set
325 (1,111 quadruplets, 82.2%), validation set (116 quadruplets, 8.6%), and test set (125 quadruplets,
326 9.2%). The distribution of roles (binder, target, off-target) played by each sequence in the full dataset
327 and individual splits can be found in Figure A4.

Table A1: SOAPi loss on training data.

| Split | Size | Loss |
|------------|------|------|
| Train | 1111 | 0.04 |
| Validation | 116 | 1.43 |
| Test | 125 | 1.57 |

Table A2: SOAPi Model Architecture and Training Hyperparameters

| Hyperparameter | Value |
|------------------------------------|---------------------|
| Model Architecture | |
| ESM Model Base | ESM2_t33_650M_UR50D |
| Embedding Dimension | 1280 |
| ESM Unfrozen Layers | 2 |
| Linear Layers | 2 |
| Positional Attention Head: n_heads | 10 |
| Adaptive Log-Sum Decoy Loss | |
| α | 5 |
| β | 0.5 |
| ϵ | 1e-8 |
| Training | |
| Max Sequence Length | 1022 |
| Batch Size / Device | 16 |
| Effective Batch Size | 128 |
| Dataloader num_workers | 30 |
| Learning Rate (LR) | 1e-4 |
| LR Scheduler: Warmup Steps | 200 |
| LR Scheduler: Total Steps | 9000 |
| LR Scheduler: Min/Max LR Ratio | 0.1 |
| Gradient Clipping | 0.5 |

| Target | Proposed sequence |
|----------------|----------------------|
| DHRSX : RPS4Y1 | EWHLAGIDNRRSLFAWELPK |

Table A3: Peptide sequence for fusion oncoprotein case study.

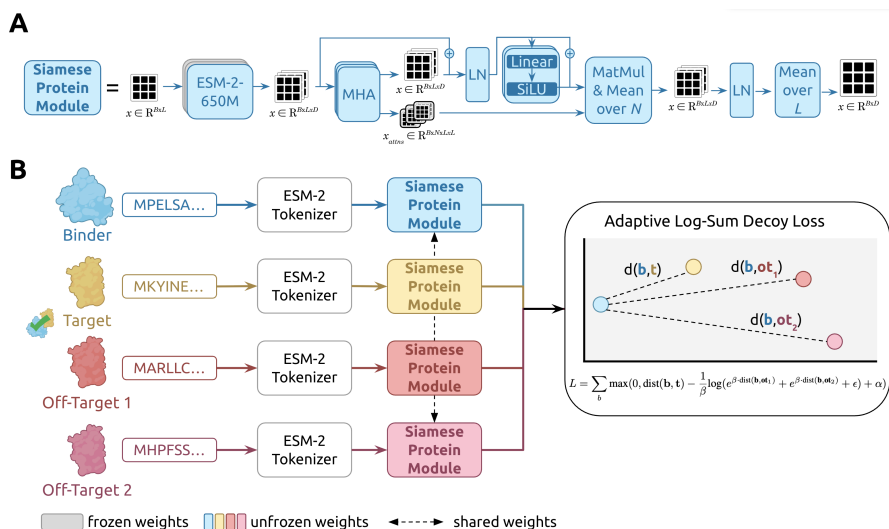


Figure A1: **SOAPI model architecture.** **A** Siamese Protein Module, the core unit of the quadruplet network. ESM-2-650M encodes sequences into $[B, 1280]$ embeddings, refined via positional attention (10 heads) with rotary embeddings, skip-connected linear layers, and attention pooling. **B** Full SOAPI pipeline. Binder, target, and off-target sequences pass through the Siamese module with shared weights. Euclidean distances between embeddings define a loss that pulls the binder toward the target while pushing it away from off-targets.

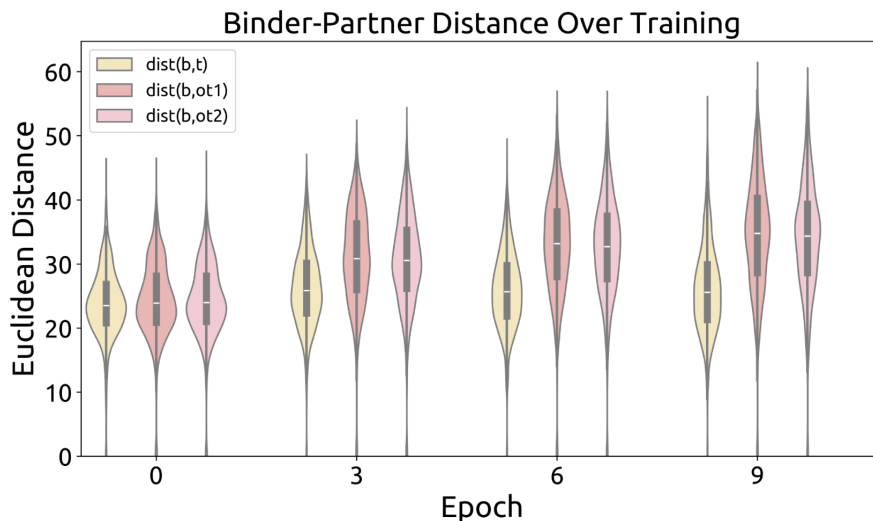


Figure A2: **Embedding separation throughout model training.** Euclidean distances between SOAPI embeddings of the proteins in each training quadruplet: $\text{dist}(\mathbf{b}, \mathbf{t})$ (binder and target), $\text{dist}(\mathbf{b}, \mathbf{ot}_1)$ (binder and off-target 1), and $\text{dist}(\mathbf{b}, \mathbf{ot}_2)$ (binder and off-target 2). The inner box of each violin plot indicates the median (white) and inter-quartile range, representing the middle 50% of distances (grey box). Distances are plotted every three epochs throughout training, starting at the end of epoch 1.

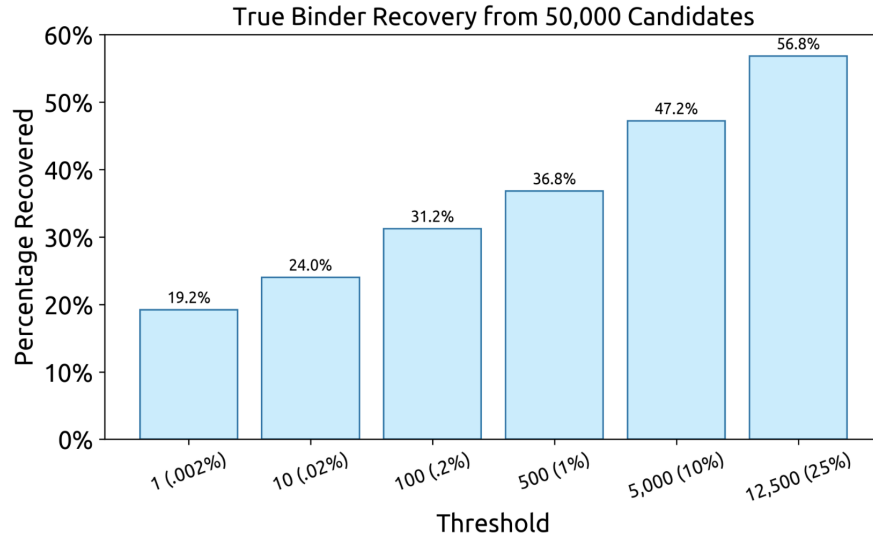


Figure A3: **SOAPI ranks true binders against 50,000 randomly generated candidates.** SOAPI produced a specificity-based ranking of 50,000 randomly generated binders and one true binder to 125 targets from the test set. Relative distance metrics D were calculated using Equation (2). Any target where SOAPI ranked the true binder among the top- N or top- $N\%$ was considered a hit. Top-1, top-10, top-100, top-1%, top-10%, and top-25% evaluations were conducted.

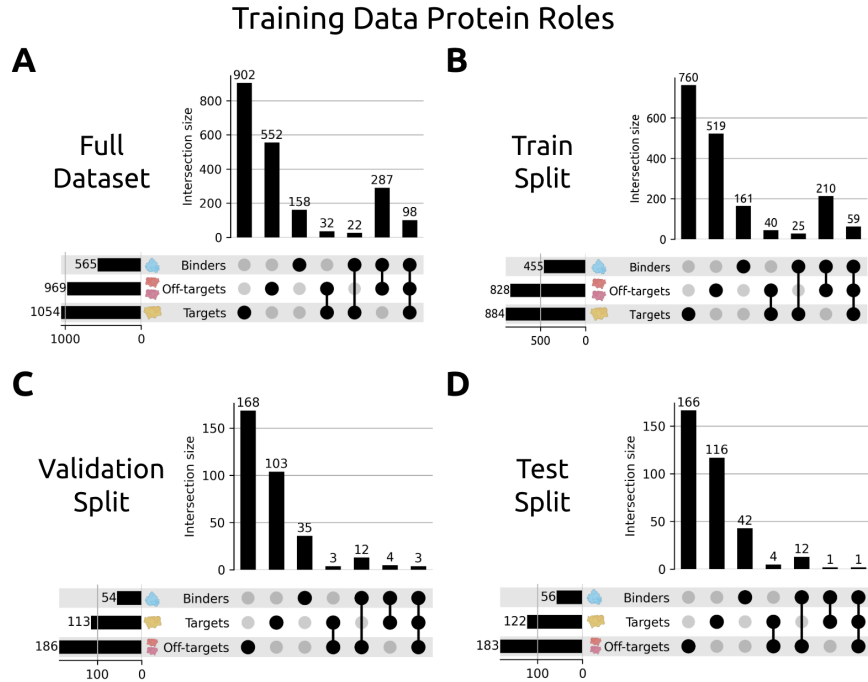


Figure A4: **Training Data Protein Roles.** Distribution of roles (binder, target, off-target) played by proteins in the quadruplets comprising the **A** full training dataset (1,352 quadruplets), **B** train split (1,111 quadruplets), **C** validation split (116 quadruplets), and **D** test split (125 quadruplets).